Reports

Observational Evidence for a Possible New Diffusion Path

BRADLEY R. HACKER* AND JOHN M. CHRISTIE

Transmission electron microscopy of experimentally deformed amphibolite suggests that submicroscopic intracrystalline tubes formed around linear defects may be a previously unrecognized kind of diffusion pathway. Deformed and compositionally altered plagioclase and amphibole crystals include moderate densities of linear defects that morphologically resemble unit dislocations but display unusual contrast. During prolonged electron irradiation, the core regions of the defects expand to well-defined tubes that are ~20 nanometers in diameter. Both observations suggest that the regions about the defect cores are glassy and were filled with silicate-water fluid during the experiments. Intracrystalline transport along these tubes would likely be several orders of magnitude faster than traditionally conceived processes of solid-state volume diffusion, grain-boundary solvent transfer, and ordinary pipe diffusion along dislocation cores.

DIFFUSION IS A FUNDAMENTAL PROCESS. In Earth materials diffusion is the rate-controlling step in many types of deformation and metamorphism. The three types of diffusion paths commonly considered are: lattice or volume diffusion, intragranular or grain-boundary diffusion, and pipe diffusion along dislocation cores. In this paper, we present evidence for a potential fourth kind of diffusion path. The evidence is largely observational and was found fortuitously during transmission electron microscope examination of amphibolite samples deformed at high pressures and temperatures.

Deformation and hydrostatic annealing experiments were performed on natural and synthetic amphibolites composed of plagioclase (30 mole percent anorthite; An_{30}), tschermakitic hornblende, and quartz (*1*). The experiments were conducted at confining pressures of 0.5 to 1.5 GPa, temperatures of 700° to 1000°C, and strain rates of 10^{-4} to 10^{-7} s^{-1} for up to 795 hours in Griggs-Blacic solid-medium apparatus. In synthetic and natural amphibolite samples heated with 1% by weight added H_2O at temperatures ≥775°C, plagioclase, tschermakitic hornblende, and quartz melted, and magnesio-hornblende and calcic plagioclase grew from the liquid (now glass). Unaltered parts of plagioclase crystals retained their original An_{30} composition, whereas altered regions had a variable composition (from An_{30} to An_{50}), depending on the conditions of the experiment.

When examined with the transmission electron microscope (TEM), these altered original crystals revealed unusual microstructures (Fig. 1). The dominant feature in Fig. 1A is a set of subparallel, glass-filled cracks. The structure between the cracks is difficult to resolve but appears to comprise a dense tangle of dislocations or stacking fault ribbons (or both). Extending outward from the crack set and also within the rest of the crystal are what appear at first observation to be unit dislocations or stacking-fault ribbons. With further scrutiny, however, these defects appear abnormal (Fig. 1B). Principally, they are anomalously wide for dislocations, which in plagioclase are typically <10 nm wide (*1*). Furthermore, the borders of some defects appear to be formed by crystallographically controlled surfaces. Stacking fault ribbons and other kinds of extended dislocations typically do not show this kind of contrast. Fringes did not appear in tilting to a variety of diffraction conditions. These unusual defects superficially resemble triple nodes formed of extended dislocations, but they are not triple nodes because they are composed of one, two, or three intersecting defects—not always three.

The images of these defects change considerably during prolonged examination in the TEM. As shown in Fig. 1C, the images of the defects and the glass-filled cracks broadened during irradiation. The material that makes up the central region or "core" of each defect appeared to be amorphous because it did not diffract. Further irradiation in the TEM led to complete vitrification and possible removal of material in the vicinity of the defects (Fig. 1D). The time required for such changes depended on the irradiation rate and, hence, the magnification and accelerating voltage.

Material clearly was removed from the foil during irradiation in the TEM (Fig. 2). Figure 2A illustrates a deformed zone in an An_{30} plagioclase crystal undergoing alteration to a more calcic composition. The bulk of the crystal contains mechanical twins and variable densities of dislocations (10^6 to 10^8 cm^{-2}). The microstructure of the deformed zone appears to consist of densely tangled dislocations, possible microcracks, and rotated crystal fragments (Fig. 2B). During further observation of the region in the electron beam, material in the deformed zone became glassy, and marked changes occurred in the images of the defects in the bulk of the crystal (Fig. 2C). Specifically, where the defects pierced the surface of the foil, material was removed from the region of the defects, and a hole formed. Parts of the defects that did not pierce the foil also changed contrast and appeared as evenly illuminated bands with sharply defined margins. The holes in the foil and the bands appeared to be tubes approximately 20 nm in diameter (Fig. 2D).

Similar defects were observed in amphibole crystals undergoing compositional change or alteration to pyroxene. Repeated attempts to induce changes in contrast of the defects in the plagioclase and amphibole crystals in the starting material with the TEM were unsuccessful. The unusual defects occurred only in deformed samples where the crystals were undergoing alteration. Specifically, they have been observed in plagioclase deformed at strain rates of 10^{-4} and 10^{-7} s^{-1} at 775°C and at strain rates of 10^{-4}, 10^{-5}, and 10^{-6} s^{-1} at 875°C, and in amphibole deformed at 875°C and at a strain rate of 10^{-6} s^{-1}. Related voids occurred in amphibole deformed at 875°C and 10^{-5} and 10^{-6} s^{-1} strain rate, and 975°C and 10^{-4} s^{-1} strain rate. We have not observed the unusual defects in plagioclase or amphibole crystals in samples that were only heated hydrostatically, although this may be an artifact of the lower defect densities of undeformed samples.

The change in defect appearance during electron irradiation in the TEM is most likely to occur in materials with low atomic number, elevated water (H_2O, OH^-, H_3O^+) content, or high silica content (*3*, *4*). Our interpretation is that the change in contrast is possible because the defects are not normal dislocations, and we suggest that the heightened rate of damage is possible

Department of Earth and Space Sciences, University of California, Los Angeles, CA 90024.

*Present address: Department of Geology, Stanford University, Stanford, CA 94305.

because the ~20-nm core region of each defect is filled with a water-silica glass that was fluid during the high-pressure and high-temperature experiments.

Inadequate thermal anchoring or electrical grounding of a TEM sample can lead to heating or charging of the sample, both of which can result in more rapid radiation damage. The samples in this study were all glued to copper grids and then coated with carbon. Because we observed the same phenomenon in different foils and in the same foils on different visits to the microscope, it is unlikely that the quality of the anchoring or the quality of the conductive coating caused the rapid radiation damage rates. It is also unlikely that the cleanliness of the foil, the cleanliness of the microscope column, or the quality of the vacuum (*3*) influenced the radiation damage rates.

It is conceivable that silica-water–filled tubes were present in the samples before irradiation. Frank (*5*) showed that dislocations with a large Burgers vector have reduced total energy if the core region dissolves to form a tube—simply because the increase in surface energy is compensated by the reduction in line energy of the dislocation. In our experiments, the increase in surface energy could also have been offset by the free energy of the reaction producing the compositional change in the plagioclase and amphibole.

To evaluate the potential importance of diffusion through 20-nm tubes, let us compare some rates of diffusion in albite. Crystals contain an equilibrium concentration of point defects that can diffuse through the lattice; hence, lattice diffusion is always a potentially important path in crystals if temperatures are high enough. Oxygen transport by lattice diffusion occurs at rates of 10^{-15} cm^2 s^{-1} at 500°C in albite (*6*). Hart (*7*) suggested that the diffusion rate through a bulk crystal containing dislocation cores was simply the sum of the rate of lattice diffusion multiplied by the area of the crystal lacking dislocation cores and the rate of pipe diffusion multiplied by the area of dislocation cores (for isotropic diffusion). For a crystal with a dislocation density of 10^9 cm^{-2}, the dislocation cores (with assumed radius of 0.5 nm) occupy an area that is $\sim 10^{-5}$ parts of the bulk crystal. Thus, for crystals with dislocation densities of $\sim 10^9$ cm^{-2}, the pipe diffusion rate must be about five orders of magnitude faster than the lattice diffusion rate in order for the pipe diffusion to contribute significantly to the rate of diffusion through the bulk crystal. Yund *et al.* (*6, 8*) have found that the pipe diffusion rate of oxygen in albite is not faster than 10^5 times the lattice diffusion rate. In other words, normal dislocations provide little enhancement of intragranular diffusion.

We can surmise that the rate of diffusion through a 20-nm intragranular tube is faster than pipe diffusion [$\sim 10^{-10}$ cm^2 s^{-1} at 500°C; (*6*)] and slower than diffusion of species in aqueous solutions [$\sim 10^{-4}$ cm^2 s^{-1}; (*9*)]. By analogy with Hart's (*7*) calculation, we can calculate the contribution of 20-nm tubes to intragranular diffusion. For a crystal with a dislocation density of 10^9 cm^{-2}, the tubes (with a radius of 10 nm)

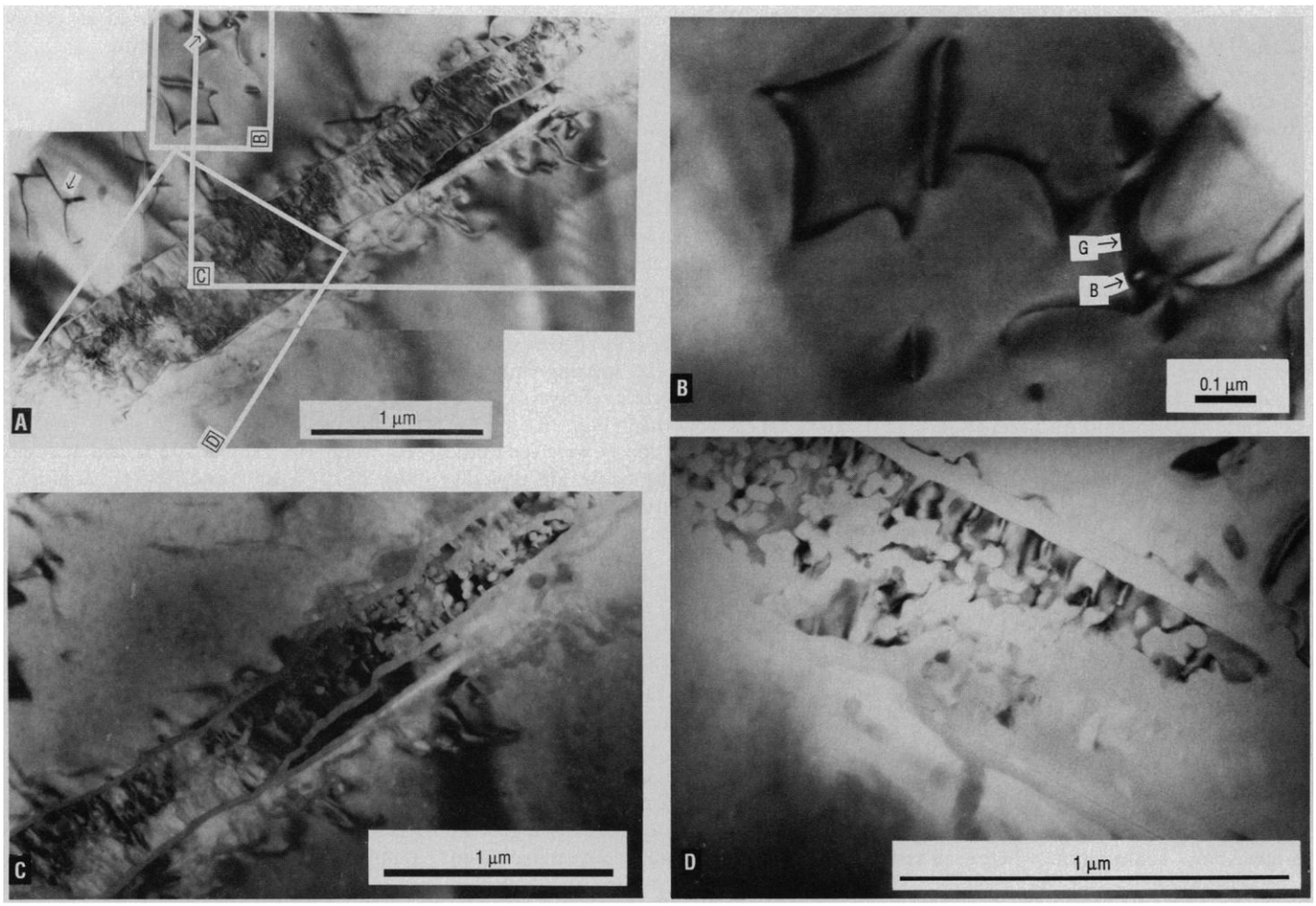

Fig. 1. Transmission electron micrographs of a planar array of defects in plagioclase. (**A**) Initial view of the array, illustrating the relatively undamaged appearance of the material. Possible crystallographic facets are marked with arrows. (**B**) Close-up of some defects with unusual contrast, showing their extended width (~50 nm) of glassy(?) material (G) and a potential bubble (B). (**C**) and (**D**) Successive views of region (A), illustrating increasing amorphization of heavily deformed region and continued production of tubes.

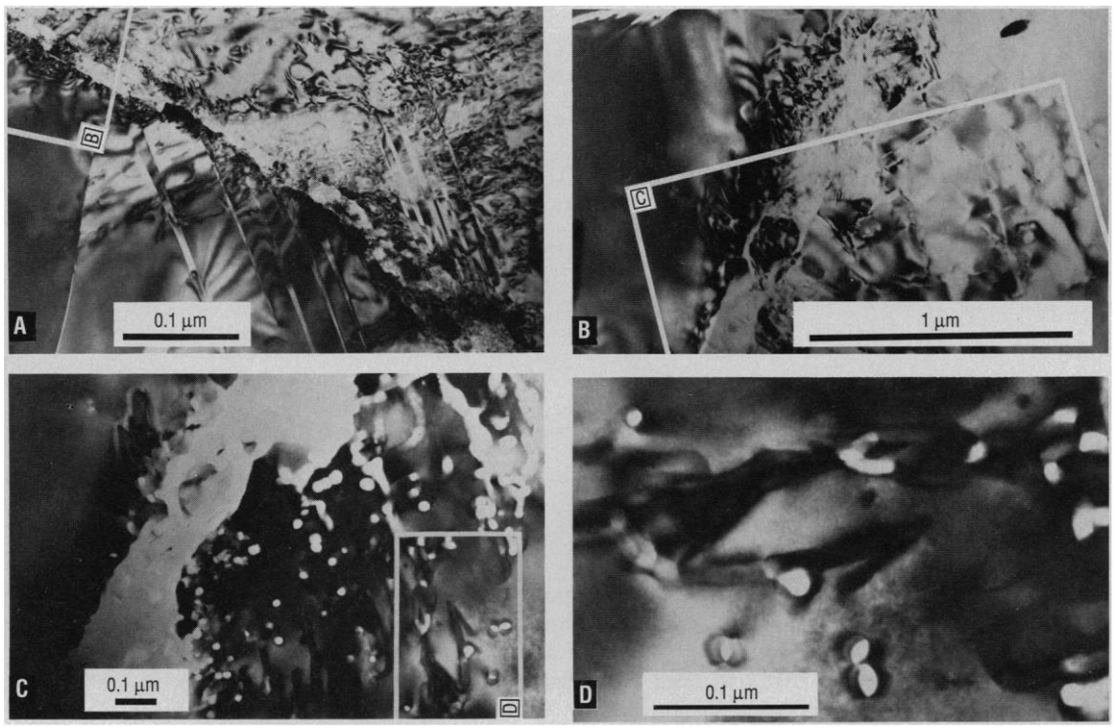

Fig. 2. (**A**) Initial view of a deformed zone, illustrating the relatively normal contrast of the dislocations and the granulated(?), though intact, nature of the interior of the zone. (**B**) Close-up of one end of the zone; little irradiation damage is yet visible. (**C**) Same region somewhat later, showing that considerable amorphization has occurred in the fault zone itself, and that the dislocations have become tubes through irradiation. (**D**) Close-up of the irradiated defects to emphasize their tube-like nature.

occupy an area that is $\sim 10^{-3}$ parts of the bulk crystal. Thus, the tube diffusion rate need only be about three orders of magnitude faster than the lattice diffusion rate for it to contribute significantly to the rate of intragranular diffusion. If the tube diffusion rate is 10^{-10} cm^2 s^{-1} (pipe diffusion rate) to 10^{-4} cm^2 s^{-1} (aqueous solution diffusion rate), the intragranular diffusion rate for a defect density of 10^9 cm^{-2} is $\sim 10^{-13}$ cm^2 s^{-1} to 10^{-7} cm^2 s^{-1}—an enhancement of intragranular diffusion rates by a factor of $\sim 10^2$ to 10^8. Conversely, if the diffusion rate for 20-nm tubes is 10^{-10} cm^2 s^{-1} (pipe diffusion rate) to 10^{-4} cm^2 s^{-1} (aqueous solution diffusion rate), an enhancement of intragranular diffusion rate by a factor of 10 can be produced by defect densities of only 10^8 cm^{-2} to 10^1 cm^{-2}. In other words, diffusion through 20-nm fluid-filled tubes has the potential to be the dominant process of intragranular diffusive mass transfer.

Veblen (*10*) suggested that structural tunnels in minerals such as zeolites and biopyriboles could facilitate chemical reactions by providing a chemical short circuit between the interior of a crystal and its surroundings. We have shown that such a short circuit might involve tubes nearly three orders of magnitude larger in cross section. Below we speculate on possible implications of these tubes for deformation and metamorphism.

If the tubes can move perpendicular to their axes by dissolution and reprecipitation—and the necessary ions can diffuse across or up and down the tube—then complete recrystallization and chemical re-equilibrium of a crystal might be achieved by migration of the defects as in dislocation slip and climb rather than by migration of a grain boundary across the entire crystal.

The tubes formed only in areas of crystal that were interpreted to be out of chemical equilibrium (*1*). Newly recrystallized parts of crystals that are near to their equilibrium composition lack tubes, although normal-looking dislocations are present. This observation implies that crystals that are further out of equilibrium may develop rapid diffusion paths to facilitate rapid recrystallization, whereas those areas of crystal that are near equilibrium may rely on more conventional diffusion paths to accomplish compositional change.

When neoblasts that are of different volume from their host crystal grow, they can produce local stresses that can cause dislocations to nucleate or move. If these dislocations then form fluid-filled tubes, the tubes may increase diffusion and enhance growth of the neoblast. This could be a self-reinforcing process wherein the production of neoblasts promotes the production of tubes and vice versa.

The stress and strain fields of a dislocation that has formed a tube are relaxed because the lattice mismatch is spread over a wider area than normal. Consequently, the behavior of these defects would be different from that of normal dislocations. A dislocation that has formed a tube may be less mobile than a normal dislocation that can move by conservative slip, because any movement of the tube must involve dissolution and precipitation of the tube walls. This reduced mobility could also cause hardening of the crystal, because mobile dislocations may pile up against the tubes. In contrast, the reduced stress and strain fields may release nearby, piled-up dislocations and allow them to glide.

Our estimates of transport rates suggest that diffusion in submicroscopic, intracrystalline tubes filled with a silicate-water fluid could be a dominant process in deformation and metamorphism under certain conditions. Anomalously rapid diffusion rates that cannot be explained by conventional diffusion paths may be related to this potential path. We caution that our observations have been made only in experimentally deformed, partially melted samples, and welcome further investigation of such defects.

REFERENCES AND NOTES

1. B. R. Hacker and J. M. Christie, *Geophys. Monogr.* **56**, 127 (1990); B. R. Hacker, *Am. Mineral.*, in press.
2. Ultra-thin foils of the deformed specimens for transmission electron microscopy were glued to copper grids and thinned by bombardment with argon ions in a Commonwealth Scientific IMMI III ion-milling machine. The gun voltage was ~5 to 6 kV, the total gun current was ≤1.0 mA and the beam current was ~15 to 35 μA. The thin foils were then coated with ~500 Å of carbon and examined at 100 keV with a JEOL JEM 100-CX TEMSCAN microscope, equipped with a beryllium double-tilt goniometer stage and a Kevex-Ray 3203-100c-VS energy-dispersive x-ray detector connected to a Tracor Northern NS-880 analysis system.
3. D. R. Veblen and P. R. Buseck, in *Proceedings of the 41st Annual Meeting of the Electron Microscopy Society of America* (San Francisco Press, San Francisco, 1983), p. 350.

4. L. W. Hobbs, in *ibid.*, p. 346.
5. F. C. Frank, *Acta Crystallogr.* **4**, 497 (1951).
6. R. A. Yund, B. M. Smith, J. Tullis, *Phys. Chem. Miner.* **7**, 185 (1981).
7. E. W. Hart, *Acta Metall.* **5**, 597 (1957).
8. R. A. Yund, J. Quigley, T. Tullis. *J. Metamorph. Geol.* **7**, 337 (1989).
9. R. C. Fletcher and A. W. Hofmann, in *Geochemical Transport and Kinetics*, A. W. Hofmann, B. J. Giletti, H. S. Yoder, R. A. Yund, Eds. (Carnegie Institution, Washington, DC, 1974), pp. 243–259; J. P. Ildefonse and V. Gabis, *Geochim. Cosmochim. Acta* **40**, 297 (1976); S. B. Tanner, D. M. Kerrick, A. C. Lasaga, *Am. J. Sci.* **285**, 577 (1985); E. H. Oelkers and H. C. Helgeson, *Geochim. Cosmochim. Acta* **52**, 63 (1988).
10. D. R. Veblen, *Geophys. Mon.* **31**, 122 (1985).
11. We thank B. Watson, T. Tingle, and two anonymous reviewers for their helpful comments. This work was funded by National Science Foundation grant EAR84-16781 to J.M.C. and a Sigma Xi research grant to B.R.H.

12 June 1990; accepted 3 October 1990

Long-Term Human B Cell Lines Dependent on Interleukin-4 and Antibody to CD40

JACQUES BANCHEREAU,* PAOLO DE PAOLI, ALAIN VALLÉ, ERIC GARCIA, FRANÇOISE ROUSSET

CD40 is a 45- to 50-kilodalton transmembrane glycoprotein expressed on B lymphocytes, epithelial cells, and some carcinoma cell lines. Human resting B lymphocytes entered a state of sustained proliferation when incubated with both the mouse fibroblastic Ltk$^-$ cell line that had been transfected with the human Fc receptor (FcγRII/CDw32) and monoclonal antibodies to CD40. In combination with interleukin-4, factor-dependent long-term normal human B cell lines were generated that were consistently negative for Epstein-Barr viral infection. Thus, cross-linking of CD40 is likely to represent an important phenomenon in the clonal expansion of B cells.

ALTHOUGH FACTOR-DEPENDENT human T cell lines and clones have been available for more than a decade, all attempts to reproducibly generate factor-dependent human B cell lines have failed (*1*), and combinations of agonistic antibodies and cytokines have essentially resulted in short-term proliferation of B cells (*2*). Here we show that interleukin-4 (IL-4) and monoclonal antibodies (MAbs) to CD40 (anti-CD40), presented in a cross-linked fashion by transfected mouse Ltk$^-$ cells that are stably expressing human FcγRII/CDw32 (*3*), permit establishment of factor-dependent long-term human B cell lines that were consistently free of Epstein-Barr virus infection.

Resting T cells strongly proliferate in response to MAbs to CD3 (anti-CD3) presented on irradiated fibroblastic mouse Ltk$^-$ cells expressing FcγRII/CDw32 (*3*) (CDw32 L cells). This proliferation results from the cross-linking of CD3 molecules on the surface of T cells after the Fc portion of the MAb binds with CDw32 (*4*). A variety of MAbs specific for various B cell surface antigens were tested for their capacity to induce the proliferation of highly purified human resting B lymphocytes cultured in the presence of irradiated CDw32 L cells (Table 1). Monoclonal antibodies 89 and G28-5, both specific for CD40, induced B cell proliferation, whereas MAbs to CD19, CD21, CD23, CD24, and CD37 did not. Monoclonal antibody 89–induced proliferation was dependent on the expression of CDw32 by L cells, since untransfected L cells or L cells transfected with HLA class I antigens did not allow MAb 89 to induce B cell proliferation (*5*). B cell proliferation occurred over a wide range of MAb 89 concentration and was maximal at 30 ng per milliliter ($\approx 10^{-10}$ M). Proliferation of B lymphocytes induced by MAb 89 + CDw32 L cells was sustained for at least 10 days after the onset of culture (Fig. 1). Thus, anti-CD40, in addition to well-known costimulatory effects on anti–immunoglobulin M (IgM)–activated B cells (*6*), can exert a direct proliferative effect on B cells when appropriately presented. Because resting B cells barely proliferate in response to soluble MAb 89, cross-linking of the CD40 antigen is probably required for B cells to proliferate. The present procedure, which is based on the use of CDw32 expressing fibroblast cells, is particularly efficient in inducing B cell proliferation, and immobilization of MAb 89 on the solid phase or cross-linking of MAb 89 with a goat antibody to mouse Ig (*5*) induced a less intense cell proliferation.

Addition of recombinant IL-4 to cultures strongly enhanced MAb 89–induced [^{3}H]thymidine incorporation (Fig. 1). In contrast, IL-2 only weakly enhanced anti-CD40–induced proliferation (*5*). Monoclonal antibody 89 induced multiplication of cultured B cells (Fig. 2A). In contrast, without MAb 89 a few viable B cells could be

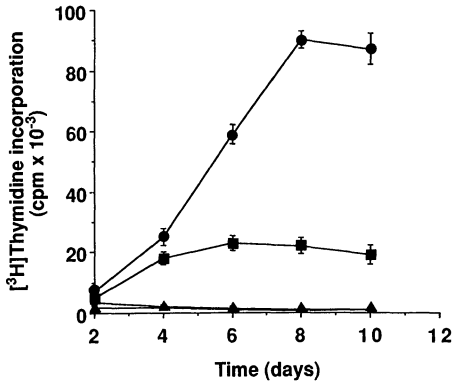

Fig. 1. Anti-CD40–induced proliferation of normal B lymphocytes is long lasting and enhanced by IL-4. Purified spleen B cells (2.5×10^4, >97% CD20+) were cultured in flat-bottom microwells for up to 10 days on 2.5×10^3 irradiated CDw32 L cells without MAb 89, without IL-4 (□); without MAb 89, with IL-4 (100 U/ml) (▲); with MAb 89, without IL-4 (■); with MAb 89, with IL-4 (100 U/ml) (●). IL-4 is a purified recombinant protein (specific activity; 10^7 U/mg) obtained from Schering-Plough Research. [^{3}H]Thymidine pulses (16 hours) were performed daily. Results are means ± SD of triplicates.

Table 1. Resting human B cells proliferate in response to MAbs to CD40 presented by CDw32-transfected L cells. Quiescent human B cells were purified by negative selection and Percoll density sedimentation from tonsils as described (*14*). B cells (10^5, 98% CD20$^+$) were cultured on irradiated (7500 rads) CDw32 L cells (10^4) in medium (*14*). Monoclonal antibodies (all IgG1, which react best with CDw32) were added to cultures at increasing concentrations (0.01 to 10 μg/ml). Only results obtained with 1 μg/ml are shown, as they are typical of the experiment. Monoclonal antibodies G28-5 and 8F1 were provided by E. A. Clark and J. F. Cantaloube, respectively. B4 was from Coulter (Hialeah, Florida) and IOB3 and IOB1 were from Immunotech (Marseilles, France). A 16-hour [^{3}H]thymidine pulse (1 μCi/well) was performed on day 3. Results are means ± SD of triplicates. ND, not determined. Results are representative of three experiments.

MAb	CD	[^{3}H]Thymidine incorporation (cpm × 10^{-3})	
		Exp. 1	Exp. 2
0		2.2 ± 0.4	1.3 ± 0.1
MAb 89	40	68.2 ± 1.4	15.0 ± 1.5
G28-5	40	ND	17.8 ± 1.3
B4	19	ND	1.3 ± 0.1
8F1	21	2.4 ± 0.5	ND
MAb 25	23	1.9 ± 0.4	ND
IOB3	24	ND	1.3 ± 0.1
IOB1	37	ND	1.2 ± 0.1

Schering-Plough, Laboratory for Immunological Research, 69571, Dardilly Cedex, France.

*To whom correspondence should be addressed.